Feline hypertrophic cardiomyopathy: reduced microvascular density and involvement of CD34+ interstitial cells

Josep M. Monné Rodríguez[1,2,3], Sonja Fonfara[1,4], Udo Hetzel[1,2], and Anja Kipar[1,2]

Abstract

The sequence of pathological events in feline hypertrophic cardiomyopathy (fHCM) is still largely unknown, although we know that fHCM is characterized by interstitial remodeling in a macrophage-driven pro-inflammatory environment and that myocardial ischemia might contribute to its progression. This study aimed to gain further insights into the structural changes associated with interstitial remodeling in fHCM with special focus on the myocardial microvasculature and the phenotype of the interstitial cells. Twenty-eight hearts (16 hearts with fHCM and 12 without cardiac disease) were evaluated in the current study, with immunohistochemistry, RNA-in situ hybridization, and transmission electron microscopy. Morphometrical evaluations revealed a statistically significant lower microvascular density in fHCM. This was associated with structural alterations in capillaries that go along with a widening of the interstitium due to the accumulation of edema fluid, collagen fibers, and mononuclear cells that also proliferated locally. The interstitial cells were mainly of fibroblastic or vascular phenotype, with a substantial contribution of predominantly resident macrophages. A large proportion expressed CD34 mRNA, which suggests a progenitor cell potential. Our results indicate that microvascular alterations are key events in the pathogenesis of fHCM and that myocardial interstitial cell populations with CD34+ phenotype play a role in the pathogenesis of the disease.

Keywords

cats, heart, hypertrophic cardiomyopathy, interstitial remodeling, microvascular alteration, progenitor stem cells

Cardiomyopathies are the most common cardiac diseases in cats.[23,61] Among these, hypertrophic cardiomyopathy (HCM) is by far the most prevalent.[76,82] Feline HCM (fHCM) is characterized by diffuse or regional increase in thickness of the left ventricular wall without chamber dilation that cannot be explained by other cardiovascular or systemic disorders.[23,24] The cause of fHCM is largely unknown; however, familial HCM has been reported in several cat populations, and 2 mutations affecting the sarcomeric myosin-binding protein C (MYBPC3) as well as 1 mutation affecting myosin-7 (MYH7) have been identified in Maine Coon, Ragdoll, and Domestic Shorthair cats, respectively.[67,68,88] This suggests that, at least in a proportion of cases, fHCM might have a genetic basis as in humans.[48] Studies on large case cohorts have shown that the disease has a higher incidence in male versus female cats and an increased prevalence with age (mean age at diagnosis: 6 years).[76,79,82] The clinical presentation is variable: some cats with HCM remain subclinical, whereas others develop congestive heart failure, thromboembolism, or sudden death.[6,25,26,37,62,80,81] This variation in presentation, as well as the fact that the pathological mechanisms associated with the development and progression of fHCM are still largely unknown, contribute to the challenges faced with clinical management of the disease.[1,61,62]

Several studies have provided information on the histopathological features of fHCM and, more recently, tried to gain some mechanistic insight into its pathogenesis.[12,44,45,50] These studies have shown that the disease is dominated by intense remodeling processes concurrent with degenerative processes in cardiomyocytes.[12,24,44,45,49,50] Our group has recently shown that fHCM is associated with a pro-inflammatory environment in which the myocardial transcription of cytokines like IL-1β and TNF-α is upregulated.[50] Remodeling processes affect both the interstitium and the contractile tissue component. The

[1]The Veterinary Cardiac Pathophysiology Consortium
[2]University of Zurich, Zurich, Switzerland
[3]University of Bern, Bern, Switzerland
[4]University of Guelph, Guelph, Ontario, Canada

Supplemental material for this article is available online.

Corresponding Author:
Anja Kipar, Institute of Veterinary Pathology, Vetsuisse Faculty, University of Zurich, Winterthurerstrasse 268, CH-8057 Zurich, Switzerland.
Email: anja.kipar@uzh.ch

interstitium was found to contain a significantly increased amount of collagen and an increased number of interstitial cells with macrophage phenotype. Smooth muscle actin–positive cells were also more numerous, which was interpreted as an increase in interstitial vessels. In addition, cardiomyocytes were multifocally replaced by patchy areas of cell-rich fibrosis with embedded macrophages and neovascularization.[50] We interpreted these as a consequence of tissue ischemia, analogous to human HCM (hHCM) where similar focal processes have also been described.[29] Interestingly, hHCM is apparently also associated with structural and functional alterations of the myocardial microvasculature (so-called microvascular dysfunction) and reduced capillary density.[15,33,40] Consequently, we hypothesized that myocardial ischemia is an intrinsic mechanistic feature of the remodeling processes in fHCM prompting an in-depth investigation of the myocardial microvasculature in fHCM hearts. The human literature also suggests that circulating stem cells play a role in the myocardial repair processes that follow ischemic insults such as coronary obstruction, and that subpopulations of macrophages, both resident and blood-derived, might play regulatory or pro-inflammatory roles in the course of an infarction process.[8,41] This suggests that blood-derived stem cells could also be relevant to the pathogenesis of fHCM.

Therefore, the present study aimed to further investigate the interstitium in the fHCM heart, to characterize any structural changes of the myocardial microvasculature and to identify the phenotype and origin (cardiac vs blood derived) of the cells involved in the remodeling processes. In addition, we wanted to gain deeper insight into the phenotypic and functional changes that cardiomyocytes undergo in fHCM. For this, we examined the hearts at light microscopic and ultrastructural levels and employed RNA in situ hybridization (RNA-ISH) and immunohistochemistry to characterize the phenotype of the cells and identify progenitor cell populations.

Material and Methods

Animals

The study was performed on the hearts of 28 cats including 16 with HCM and 12 controls. All animals had undergone a full diagnostic postmortem examination within 24 hours after death, upon the owners' request (HCM cats), and as part of a study protocol (control cats; see below). The 16 animals with HCM were of different breeds, with 3 intact males, 10 neutered males, 1 intact female, and 2 spayed females (Supplemental Table S1). HCM cats had a mean age of 8.6 ± 4.1 years (mean ± standard deviation) and a mean body weight of 5.2 ± 1.2 kg (Supplemental Table S1). Nine cats (cases 4, 6, 7, 9, 12–16) had been clinically diagnosed with HCM by a specialist in veterinary cardiology by means of echocardiography; of these, one was identified as end-stage HCM (case 14) based on thinning and hypokinesis of the left ventricular free wall on echocardiography, whereas the other cats had interventricular septum and/or left ventricular free wall thickening (>6 mm in

diastole). Seven cats had died without a clinical diagnosis of fHCM. Of these 7 cats, 3 were presented with sudden death (cases 1, 8, and 11) and 4 (cases 2, 3, 5, and 10) with clinical signs of respiratory distress. In all animals, HCM was confirmed by the postmortem examination, which revealed an obvious thickening of the left ventricular walls and narrowing of the ventricular lumen.

The mean heart weight (HW) of the fHCM cases was 29.6 ± 7.2 g (mean ± standard deviation), the mean HW/BW (%) was 0.53 ± 0.25 (reference values 0.28 ± 0.88).[84] The histological findings were consistent with those previously described for fHCM.[50] Cats with a subjectively thickened left ventricular wall with histological evidence of interstitial fibrosis and/or cardiomyocyte degeneration and disarray were included in the study (Supplemental Table S2). One cat had a saddle thrombus in the caudal abdominal aorta (case 4) and had presented clinically with paresis of the hind limbs; another had a thrombus in the left ventricle (case 7). Two cats had an unrelated concomitant pathological process, that is, a necrotizing bronchopneumonia the cause of which could not be identified (case 2) and an ependymoma (case 6).

Twelve control hearts were included. Of these, 11 were from 1.5-year-old healthy Domestic Shorthair cats (6 male, 5 female; cases C1–C11) that had served as control animals in an experimental study undertaken by a commercial provider. Upon postmortem examination, these animals did not exhibit any pathological changes. Also included was the heart of a 7-year-old female neutered Domestic Shorthair cat (case C12) that had been euthanized for behavioral reasons.

Sampling, Histological and Immunohistological Examinations

Hearts were removed as part of the routine necropsy and macroscopically examined for any pathological changes, dissected following the inflow-outflow method,[84] or sectioned longitudinally to correspond to the 2-dimensional long axis echocardiographic view to visualize the 4 cardiac chambers.[63] After removing the pericardium and any clotted blood in the chambers, the heart was weighed and fixed in 4% neutral buffered formalin for 48 to 72 hours. Transverse sections (including left and right ventricular free wall and interventricular septum) of the mid ventricle were prepared. In order to assess the structural changes in a second plane of section, one longitudinal section encompassing the ventricular free walls with atrium and atrioventricular valves was additionally prepared in 4 HCM cases (cases 12–15).

The tissue specimens were routinely embedded in paraffin wax. Consecutive sections (3–5 μm) were prepared, routinely stained with hematoxylin-eosin (HE), and subjected to immunohistochemistry and RNA-in situ hybridization. HE-stained sections served for the general assessment of cardiomyocyte, interstitial, and focal changes.[50]

Immunohistochemistry was performed using an AutostainerLink48 (Agilent Technologies, Inc) or the Discovery XT

autostainer (Ventana Medical System, Inc). It served to detect apoptotic cells (cleaved caspase 3+) and proliferating cells (Ki67+), endothelial cells (CD31+), smooth muscle cells (α-smooth muscle actin [α-SMA]+), macrophages (Iba1+; calprotectin+), cardiac stem cells, and mast cells (c-Kit+) in all cases. Staining for procollagen I, collagen I, and collagen IV was applied in selected cases to further characterize dense patchy collagen depositions. Antibodies with antigen retrieval and detection methods are listed in Supplemental Table S3. Briefly, after deparaffinization, antigen retrieval was performed for all antigens except for α-SMA, by incubation of the slides with citrate buffer (pH 6) at 98 °C for 20 minutes (calprotectin, Iba1, Ki67, procollagen I) or 80 °C for 20 minutes (collagen I), EDTA buffer (pH 9) at 98 °C for 20 minutes (CD31 and collagen IV), or Cell conditioning 1 (CC1; Ventana Medical Systems; cleaved caspase 3) at 98 °C for 20 minutes. Endogenous peroxidase was blocked by incubation with hydrogen peroxide (Agilent) solution for 10 minutes, followed by incubation with REAL Antibody Diluent (Agilent) for 30 minutes at room temperature (RT). DAB substrate buffer (Agilent) was used as detection chromogen. Slides were then incubated with the primary antibodies and matching secondary antibodies, using the appropriate detection system (Supplemental Table S3). Sections were washed with phosphate buffered saline (pH 8) between each incubation step. Finally, sections were counterstained with hematoxylin for 40 seconds and coverslipped. Sections stained for CD31 were subsequently stained with the van Gieson stain to highlight the interstitial collagen deposition. Sections from the following tissues served as positive controls: lymph node (Ki67, cleaved caspase 3, Iba1, calprotectin), skin (procollagen I, collagen I, collagen IV, α-SMA), and lung (CD31). Consecutive sections incubated without the primary antibody served as negative controls.

RNA-In Situ Hybridization (RNA-ISH)

For RNA-ISH, the RNAscope (Advanced Cell Diagnostics Inc [ACD]) technology was applied. A series of target oligoprobes were designed by the manufacturer to hybridize a range of specific feline gene transcripts that can be regarded as markers for stem cell subsets and monocyte or vascular cell origin or are involved in cell signaling and hypertrophy (Table 1): Nanog, Octa-4, CD34, Kit, C-C chemokine receptor 2 (CCR2), CD14, CD29, CD34, CD133, Kit, collagen type I alpha 1 chain (Col1A1), myocyte-specific enhancer factor 2C (MEF2C), platelet derived growth factor receptor beta (PDGFRB), and vascular endothelial growth factor 2 (VEGFR2). A protocol for manual staining was applied, following the manufacturer's instructions. Briefly, sections were dried for 1 hour at 60 °C and dehydrated in a series of graded alcohols and xylene. Following standardized pretreatment steps with RNAscope Pretreatment Reagents (RNAscope Hydrogen Peroxide Reagent: 10 minutes at RT; RNAscope Target Retrieval Reagent: 15 minutes at 100 °C; RNAscope Protease Plus Reagent: 30 minutes at 40 °C), sections were incubated with the oligoprobes for 2 hours at 40 °C in a HybEZ Oven.

RNAscope 2.5 HD Reagent Kit-BROWN was used for the amplification and detection steps (incubation with reagent [1] for 30 minutes at 40 °C; reagent [2] for 15 minutes at 40 °C; reagent [3] for 30 minutes at 40 °C; reagent [4] for 15 minutes at 15 °C, reagent [5] for 30 minutes at RT; reagent [6] for 15 minutes at RT; and DAB-B for 10 minutes at RT). Slides were counterstained for 60 seconds with hematoxylin and mounted. A soft tissue sarcoma served as positive control for Nanog and Octa-4 mRNA, a lymph node for CD14 and CD34, bone marrow for CCR2, the thyroid gland for VEGFR2, PDGFRB, and Kit, the pancreas for CD133, and the cerebral cortex for MEF2C mRNA.

Oligoprobes specific for feline PPIB (Cyclophilin B) mRNA were used as positive control to confirm the correct technical approach and to assess the RNA quality of the samples (positive brown dots in interstitial cells visible at 200× magnification and >5 dots per cardiomyocyte with more than 50% of cardiomyocytes positive). Oligoprobes specific for the DapB gene of the *Bacillus subtilis* strain SMY were used as a negative control.

The positive signal for the markers of interest was represented by individual brown dots within the cells; accordingly, the signal intensity was assessed based on the number of dots per cell in a 400× magnification and considered as weak (up to 3 dots in interstitial cells and up to 10 dots in cardiomyocytes), moderate (4–10 dots in interstitial cells and 11–20 dots in cardiomyocytes), or strong (clusters of dots in interstitial cells and more than 20 dots in cardiomyocytes).

Transmission Electron Microscopy (TEM)

Additional fresh myocardial samples were collected for TEM within 1 hour of death from 6 HCM cases (cases 4, 7, 10, 12–15; Supplemental Table S1) and 1 control heart (case C12). The samples were fixed for 24 hours in 5% glutaraldehyde, buffered in 0.2 M cacodylic acid buffer, pH 7.3, trimmed, and routinely embedded in epoxy resin. Toluidine blue–stained semithin sections (1.5 μm) were prepared to select areas of interest for the preparation of ultrathin sections (75 nm) that were contrasted with lead citrate and uranyl acetate and viewed with a Philips CM10, operating with a Gatan Orius Sc1000 digital camera (Gatan Microscopical Suite, Digital Micrograph).

Morphometric Analyses

Slides were scanned (NanoZoomer-XR C12000; Hamamatsu) and evaluated with an image analysis software (Visiopharm 2020.08.1.8403; Visiopharm). For the quantification of interstitial capillaries, 20 square-shaped regions of interest (ROIs) of 0.09 mm^2 were manually annotated in a random manner in areas where cardiomyocytes were transversely cut (subendocardial and subepicardial regions) and did not exhibit any focal areas of cell-rich fibrosis (Suppl. Fig. S1). Subsequently a threshold classification method with a DAB filter was used for the detection of vascular structures, based on the expression of CD31, and for the extent of interstitial edema and collagen deposition, based on the

Table 1. Cell markers detected by RNA-in situ hybridization, cells known to express the markers and their functions.[a]

Marker	Cells known to express the marker and its functions
CCR2	C-C chemokine receptor 2. Chemokine receptor of monocyte chemoattractant protein-1 (MCP-1). Myocardium: contains CCR2− and CCR2+ macrophages. CCR2− macrophages: derived from primitive yolk sac and fetal monocyte progenitors, self-maintained in the heart independently from the bone marrow; regenerative functions. CCR+ macrophages: maintained through gradual monocyte recruitment and local proliferation; pro-inflammatory functions.[9,27,36]
CD14	LPS receptor. Humans: expression in monocytes, with variable intensity depending on monocyte subset (ie, classical, nonclassical, and intermediate monocytes) and macrophages;[27] cultured circulating CD14+ monocytes differentiate into mesenchymal and endothelial lineages, so-called monocyte-derived multipotential cells.[54] Cats: expression in proportion of monocytes in bone marrow and peripheral blood; cultured dendritic cells.[5,28] Myocardium (humans): contains CD14+ macrophages.[9]
CD29	Cell surface receptor with roles in cell adhesion and migration, and regulation of cellular phenotype.[86] Myocardium: receptor for different extracellular matrix proteins including collagens, involved in myofibroblast differentiation and facilitation of interaction between cardiomyocytes, fibroblasts, and endothelial cells;[86] also known to be involved in cardiac remodeling and fibrosis as well as cardiac hypertrophy.[18] Cats: CD29 expression found in cultured cardiomyocytes, bone marrow cells, fibroblasts of the renal cortex, and adipose tissue derived mesenchymal stem cells.[5,46,56,100]
CD34	Transmembrane phosphoglycoprotein expressed in hematopoietic stem cells, hematopoietic progenitor cells, and wide range of non-hematopoietic stem cells including mesenchymal stem cells and endothelial progenitor cells.[66,90] Function largely unknown but regulation of cell stemness and proliferation, cell adhesion, and hematopoietic cell trafficking is suggested.[66,90] Myocardium: expressed by various endogenous cardiac stem cells with cardiogenic or vascular phenotype,[30] and by interstitial Cajal-like cells (so-called telocytes).[52] Cats: protein expression in endothelial cells of renal capillaries and various tumors, progenitor cells from the umbilical cord;[14,39,72] mRNA expression in different organs (ie, brain, spleen, heart, testis, thymus, liver) with highest levels in the heart (no information on cellular source).[103]
CD133	Membrane glycoprotein expressed by wide range of stem cells, cancer stem cells, and differentiated cells (mainly polarized epithelial cells, glial cells, and photoreceptors).[11,34] Function: not clear; involved in maintenance of the plasma membrane in differentiated epithelial cells; linked to molecular pathways associated with cell proliferation, angiogenesis and migration in cancer cells. Humans: used as a marker of circulating endothelial progenitor cells, together with CD34 and VEGFR2.[41,97] Cats: used as a marker for cancer stem cells.[77,78]
KIT	Tyrosine kinase receptor expressed in several cell types including germ and hematopoietic stem cells, mast cells, melanocytes, and Cajal interstitial cells.[69] Function: activation of various transcription factors involved in apoptosis, cell differentiation, proliferation, chemotaxis, and cell adhesion.[69] Myocardium: expression by cells regarded as cardiac stem cells (humans, mice, cats)[30,35,93,104] and by telocytes.[52]
Col1A1	Collagen type 1 alpha 1 chain. Gene encoding the α chain of type I collagen; expressed by fibroblasts.[42]
MEF2C	Myocyte enhancer factor 2C. Transcription factor with central roles in embryological differentiation and morphogenesis of cardiac, skeletal, and smooth muscle cells, the nervous system and B cells. Myocardium: promotes cardiac hypertrophy upon pathological stimuli; genetic variants leading to increased MEF2C expression have been described in human HCM.[3,4,16]
Nanog	Transcription factor expressed in embryonic stem cells to maintain cell pluripotency.[70] Myocardium: cardiac stem cell marker in rat and mouse.[59,101] Cats: identified in amniotic epithelial cells and mesenchymal stem cells; used as transcription factor to generate induced pluripotent stem cells.[20,46,87,105]
Oct4	Transcription factor expressed by embryonic stem cells to maintain cell pluripotency.[95] Myocardium: cardiac stem cell marker in rat and mouse.[101,102] Cats: identified in amniotic epithelial cells and mesenchymal stem cells; used as transcription factor to generate induced pluripotent stem cells.[20,46,87,105]
PDGFRB	Platelet derived growth factor receptor beta. Cell-surface receptor with tyrosine kinase domain, expressed in vascular smooth muscle cells and pericytes.[43] Myocardium: expressed by telocytes.[52] Functions: role in maintenance of vasculature homeostasis,[43] regulation of angiogenesis by mediating pericyte and vascular smooth muscle cell migration for stabilization of newly formed vessels.[2] Cats: expression in normal endocrine pancreas and endothelial cells and histiocytic cells in histiocytic disorders.[96]
VEGFR2	Vascular endothelial growth factor receptor 2. Transmembrane receptor with tyrosine kinase domain, expressed in endothelial cells and endothelial progenitor cells.[41,97] Functions: role in vascular permeability and angiogenesis; promoting proliferating, differentiation, and sprouting of endothelial cells during angiogenesis.[2] Cats: expressed by neoplastic cells in renal cell carcinoma and mammary cell carcinoma.[13,73]

[a]Unless specifically stated, the information originates from studies in mice and humans.

presence of empty spaces and the van Gieson staining reaction. Results were quantified as vessels per mm^2 and percentage of clear spaces (edema), respectively. For the quantification of Ki67, Iba1, and calprotectin positive cells, a first tissue detection application using a Decision Forest classification method was used to outline an entire cross section of the left ventricular free wall (6 mm width), which was defined as ROI. Subsequently, a threshold classification method with a DAB filter was used for the detection of positive cells; cells expressing each marker were quantified as positive cells per mm^2.

Statistical Analysis

Data from morphometric measurements were analyzed using the commercially available software package (IBM SPSS Statistics 21). Basic descriptive statistics (mean, median, variance, standard deviation, interquartile range, and confidence interval) were calculated for the morphometrical variables recorded. Distribution of data was analyzed applying graphical Q-Q plots, Kolmogorov-Smirnov, and Shapiro-Wilk analyses. Data for Iba1, Ki67, and calprotectin were not normally distributed and were log-transformed to improve normality and the model assumptions necessary for parametric analysis. Results obtained from the 2 groups were compared using unpaired t tests. Statistical significance was defined as $P < .05$.

Results

The main histological features were consistent with those previously described for fHCM.[12,24,44,45,50] Structural changes affecting the interstitial compartment and cardiomyocytes were subsequently focused upon.

In Feline HCM, the Capillary Density Is Reduced Within the Myocardium, With Structural Alterations of the Microvasculature

In HCM hearts, compared to control hearts, the interstitium was significantly widened, with clear spaces, variable but comparatively increased amounts of spindle-shaped and round cells compatible with macrophages, as well as partly densely packed collagen fibrils as shown by the van Gieson stain and immunohistochemistry for collagen I (Figs. 1, 2; Suppl. Fig. S2). As a consequence, the vascular density (ie, the number of CD31+ endothelial cells forming ring-shaped capillary structures/mm^2) was significantly lower than in control hearts (Table 2). Capillaries were irregularly arranged, formed tortuous branches, and often had plump endothelium (Fig. 3). Some had thickening of the vascular basement membrane, as revealed by the increase in collagen IV protein expression (Fig. 4). None of these features were seen in the control hearts in which capillaries were arranged parallel to the cardiomyocytes with one capillary placed in a straight line between 2 cardiomyocytes (Suppl. Fig. S3). Ultrastructural analysis confirmed the vascular alterations, supported by the following findings: Capillaries occasionally formed tight curves and there was branching (Fig. 5). Capillaries were often lined by plump reactive endothelial cells with fluid accumulation in the cytoplasm and an irregular course of the luminal plasma membrane, resulting in narrowing of the capillary lumen (Figs. 5, 6). Some capillaries were surrounded by rows of round and plump pericytes,[7] and in some the basement membrane was thickened. None of these features was observed in the control animal (Figs. 5, 6). The interstitium was expanded by ample intercellular spaces that contained amorphous electron-lucent material consistent with edema fluid (Figs. 5–7). There were areas that showed moderate to large amounts of collagen fibrils that formed irregular bundles;

these were either admixed with edema fluid or formed dense fibrous connective tissue with embedded spindle-shaped cells interpreted as fibroblasts (Figs. 5–7). The accumulation of fluid and collagen resulted in marked expansion of the distance between capillaries and cardiomyocytes.

In addition, 9 cases (cases 1, 3, 5, 8, 12–16) showed changes in medium-sized myocardial arteries characterized by thickening of the tunica media with narrowing of the vascular lumen either due to expansion of the media by hypertrophic smooth muscle cells or widening due to pale eosinophilic material, interpreted as collagen, that replaced the smooth muscle cells as confirmed by loss of staining for α-SMA (arteriosclerosis; Fig. 8).

In Feline HCM, the Myocardial Interstitium Contains Proliferating Cells and an Increased Amount of Cells With Fibroblast and Vascular Phenotypes

In the attempt to gain information on the origin of the cells that we observed in increased numbers in the interstitium, we examined the myocardium for the transcription of CD34, VEGFR2, PDGFRB, CD133, Kit, and Col1A (Table 1).

In control animals, the myocardium exhibited small to moderate numbers of interstitial cells with a weak CD34 and VEGFR2 mRNA signal; their arrangement and morphology was consistent with endothelial cells of interstitial capillaries (Suppl. Figs. S4a, S5). A weak endothelial CD34 mRNA signal was also seen in small to medium-sized vessels (Suppl. Fig. S4b) but there was no VEGFR2 signal. Scattered medial smooth muscle cells and adventitial pericytes were PDGFRB mRNA-positive (Suppl. Fig. S6a), and so were scattered individual cells in the interstitium (Suppl. Fig. S6b). There were small to moderate numbers of interstitial cells with weak to moderate Col1A1 mRNA signal, interpreted as fibroblasts. Immunohistochemistry showed cytoplasmic procollagen I expression in small numbers of fibroblasts and a few collagen I bundles in the interstitial space (Suppl. Figs. S7–S9). Rare elongate to spindle-shaped interstitial cells expressed Kit mRNA, while Kit protein was not detected (Suppl. Fig. S10). There were no CD133 mRNA-positive cells.

In HCM, small to medium-sized myocardial vessels and interstitial capillaries showed a similar transcription pattern as in control hearts. The interstitium contained variable amounts of spindle-shaped or slightly plumper cells of which moderate to large numbers were found to moderately to strongly transcribe CD34 (Fig. 9). There were also moderate to large numbers of cells that strongly transcribed Col1A1 (Fig. 10), and similar numbers showing procollagen I protein expression in the cytoplasm (Fig. 11). In line with this was the presence of abundant collagen in the extracellular interstitial space; this was identified as collagen I and mildly increased amounts of collagen IV compared to control animals (Fig. 2). In addition, there were small numbers of cells that transcribed VEGFR2 (Fig. 12) and/or PDGFRB (Fig. 13). Occasionally, CD34,
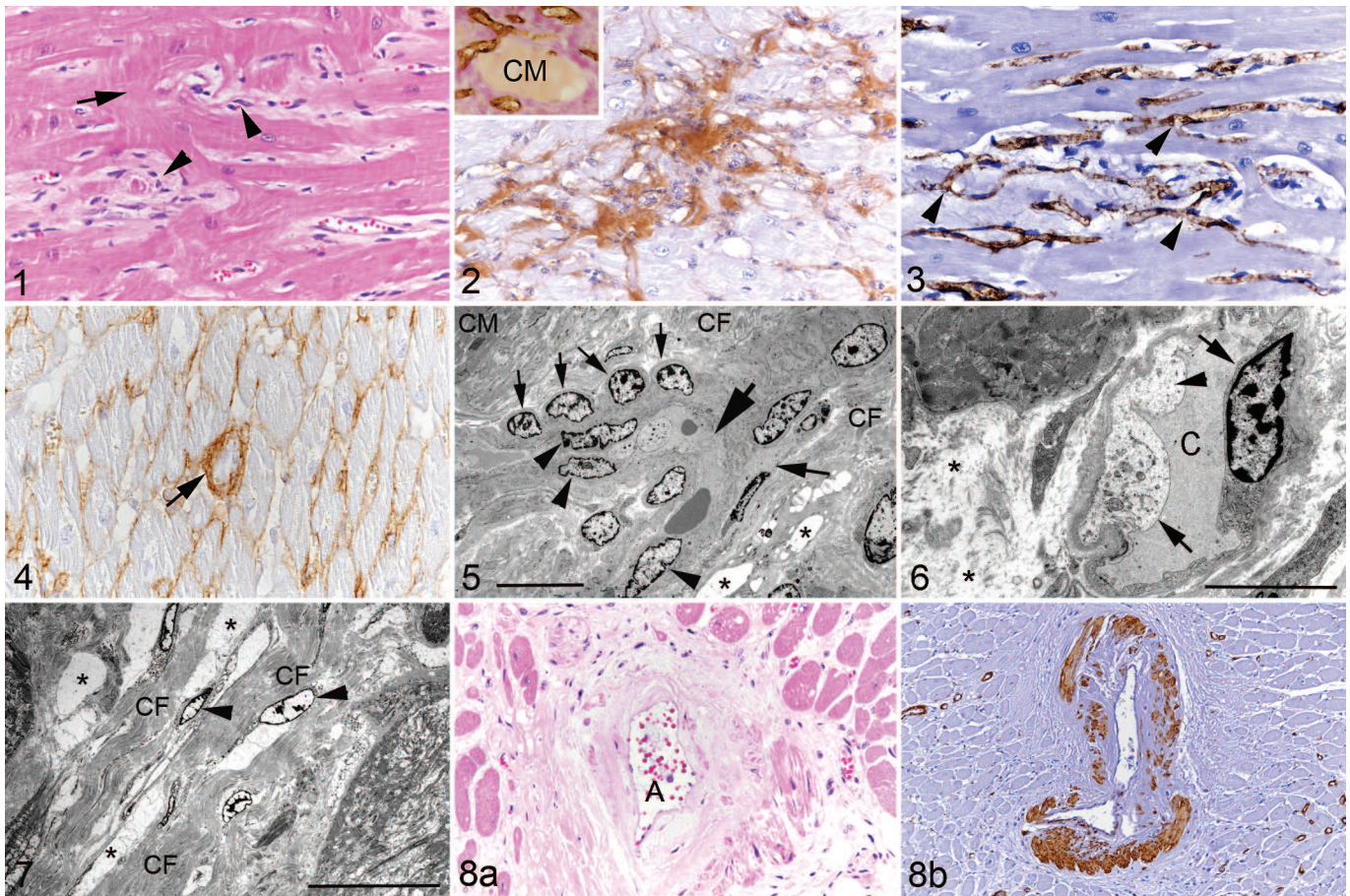
Figures 1–8. Hypertrophic cardiomyopathy, left ventricular free wall, cat. **Figure 1.** Case 8. There is widening of the interstitium with increased numbers of interstitial cells (arrowheads) and cardiomyocyte disarray (arrow). Hematoxylin eosin (HE). **Figure 2.** Case 13. The widened interstitium contains abundant collagen I. Immunohistochemistry (IHC). Inset: Collagen deposition (pink) is present in the interstitium between blood vessels (brown). IHC for CD31 (microvasculature) with van Gieson counterstain. CM: cardiomyocyte. **Figure 3.** Case 6. Myocardial capillaries are irregularly arranged and appear to branch frequently (arrowheads). IHC for CD31. **Figure 4.** Case 12. The interstitium contains fine strands of collagen IV. Occasional small capillaries exhibit thickening of the basement membrane due to abundant collagen IV deposition (arrow). IHC. **Figure 5.** Case 13. Interstitium with a capillary forming a tight curve (large arrow). There is also evidence of branching (medium sized arrow on the right). The nuclei of the lining endothelial cells are relatively plump (arrowheads). Aligned with the capillary is a row of plump pericytes (small arrows). The interstitium is expanded by edema fluid (represented by electron-lucent, amorphous material filling well-demarcated intercellular spaces; asterisks) and irregularly arranged collagen fiber bundles (CF). CM: cardiomyocyte. Transmission electron microscopy (TEM); bar = 10 μm. **Figure 6.** Case 15. Interstitial capillary (C) with narrowing of the lumen, lined by swollen endothelial cells (arrows) with irregular luminal surface and fluid accumulation in the cytoplasm (arrowhead). The interstitium is distended (edema; asterisks). TEM; bar = 5 μm. **Figure 7.** Case 12. The interstitium is severely expanded due to abundant collagen fiber bundles (CF) and edema fluid containing amorphous electron-lucent material (asterisks). There are some embedded fibroblasts (arrowheads). TEM; bar = 20 μm. **Figure 8.** Case 5. Arteriosclerosis of a myocardial artery. (a) Affected artery (A) with diffuse thickening of the tunica media by eosinophilic amorphous material (collagen). HE. (b) Deposition of the proteinaceous material is associated with focal loss of smooth muscle cells in the tunica media and narrowing of the arterial lumen. IHC for α-smooth muscle actin.

VEGFR2, and PDGFRB mRNA-positive cells were not only found in small capillaries but were also seen to aggregate as rudimentary ring-shaped structures resembling primitive vessels (Figs. 9, 12, and 13). There was no evidence of CD133 transcription, as in control hearts.

Labeling for Ki67 (as a marker of proliferation) showed nuclear positive expression in some round macrophage-like and spindle-shaped cells as well as occasional endothelial cells of differentiated capillaries (Fig. 14). The number of Ki67-positive cells was significantly higher in the HCM hearts compared to control hearts which only showed rare positive interstitial cells (Table 2).

We also investigated the transcription of markers associated with signaling transduction pathways in stem cells (Table 1). Neither Nanog nor Oct-4 were transcribed in HCM, but there were rare to few individual spindle-shaped cells that expressed Kit mRNA, and rare individual cells that showed Kit protein expression in the cytoplasm (Fig. 15). Small numbers of interstitial cells exhibited a weak MEF2C signal (Fig. 16). In control hearts, rare individual spindle-shaped interstitial cells

Table 2. Overall cellular and interstitial composition of the left ventricular myocardium in 12 control cats and 16 cats with hypertrophic cardiomyopathy (HCM).[a]

Parameter	Control (*n* = 12)	HCM (*n* = 16)	*P*
CD31 (n/mm^2)[b]	2342.38 ± 417.11	1686.18 ± 241.4	<.001
Interstitium (edema)[c]	0.38 ± 0.19	5.84 ± 3.96	.002
Interstitium (collagen)[c]	1.22 ± 0.95	2.9 ± 1.9	.012
Ki67 (n/mm^2)[d]	1.32 ± 1.62	19.49 ± 19.79	<.001
Iba1 (n/mm^2)[d]	6.36 ± 3.80	64.48 ± 73.19	<.001
Calprotectin (n/mm^2)[d]	3.11 ± 3.10	16.21 ± 24.02	.541

[a]The data show the mean ± standard deviation based on the morphometric evaluation of histological and immunohistochemical specimens.
[b]Number of capillaries (n/mm^2) based on the number of CD31-positive endothelial cells in 20 square regions of interest (ROI) of 0.09 mm^2.
[c]Percentage of myocardium composed of interstitial edema or interstitial collagen (Van-Gieson stain: positive) in 20 square regions of interest (ROI) of 0.09 mm^2.
[d]Number (n/mm^2) of positive cells in an entire cross section of the left ventricular free wall (6 mm width).

exhibited a weak Kit mRNA signal (Suppl. Fig. S10), and/or a weak MEF2C mRNA signal (Suppl. Fig. S11). Nanog or Oct4 mRNA-positive cells were not detected in control hearts.

Cell death was minimal among the interstitial cells and restricted to rare individual apoptotic cells in the HCM myocardium, as confirmed by staining for cleaved caspase 3.

The vast majority of interstitial cells also showed a strong CD29 (β$_1$-integrin) mRNA signal (Fig. 34). The equivalent cells in control hearts were also positive, though with only weak to moderate signal intensity (Suppl. Fig. S12).

The Focal Myocardial Areas of Cell-Rich Fibrosis in HCM Are Similar in Composition to the Interstitium

In 7 HCM hearts (cases 1, 7–9, 12–14) the sections also contained focal areas of cell-rich fibrosis (Fig. 17) consistent with those previously described by our group.[50] These areas of cardiomyocyte replacement by spindle cell infiltrates and new blood vessels of variable caliber embedded in a collagenous matrix had a lot in common with the interstitial changes described above. They comprised a moderate number of cells showing moderate to strong CD34 and/or Col1A1 transcription (Figs. 18, 19). Lesions with abundant collagen (ie, collagen I and IV) deposition (Fig. 20) and lower cellularity contained only few cells with moderate Col1A1 transcription. When abundant vessels were present, there was substantial collagen IV expression in the basement membranes (Fig. 21). The embedded small vessels were composed of endothelial cells (CD31+) of which small numbers showed weak to moderate CD34 (Fig. 18), VEGFR2, and/or PDGFRB mRNA signals. Small numbers of spindle-shaped cells transcribed MEF2C (Fig. 22), and scattered cells expressed Kit mRNA (Fig. 23). The lesions also contained occasional mast cells, as shown by light microscopy in combination with Kit mRNA and protein expression (Fig. 23).

There were a few proliferating (Ki67+) spindle-shaped cells and rare apoptotic (cleaved caspase 3+) cells.

## The Interstitial Macrophage Accumulation in Feline HCM Is Not the Consequence of Monocyte Recruitment

We have previously identified a significantly increased macrophage (Iba1+) population in the interstitium,[50] and have now attempted to identify their origin from resident cardiac populations or monocytes. Staining of the present case cohort for Iba1 confirmed that positive cells were present in significantly higher numbers (approximately 10 times higher) in the HCM myocardium than in control hearts (Table 2). Calprotectin-positive macrophages (representing recently blood-derived macrophages)[92] were also observed in fHCM and control animals, and while there was a trend for higher numbers in the fHCM group (5 times higher in fHCM compared to controls), there was not a significant difference (Table 2). RNA-ISH for CD14 (Fig. 24), a marker expressed in some populations of circulating monocytes and macrophages, and CCR2 (Fig. 25), confirmed as a marker of monocytes and recently blood-recruited macrophages in humans,[27] confirmed the calprotectin results as only rare cells with a moderate mRNA signal were observed. Cells positive for either marker were not detected in the interstitium of the control hearts.

The focal cell-rich fibrotic lesions also contained variable numbers of Iba1+ macrophages and a few calprotectin-positive and CD14 mRNA positive cells and exhibited scattered cells that showed CCR2 transcription. In 2 animals (cases 1 and 12), the focal lesions also contained small clusters (up to 15 cells) of CD14-positive and fewer CCR2 mRNA-positive round and spindle-shaped cells (Figs. 26, 27).

In HCM, Cardiomyocytes Undergo Degeneration But Also Exhibit Limited Phenotypic Changes

Degenerative changes (cytoplasmic vacuolation and loss of striation, as well as necrosis of individual cardiomyocytes) mainly close to areas of fibrosis have previously been described in fHCM.[24,50] These were regularly seen in the present case cohort (Figs. 1, 28). There were also rare randomly distributed apoptotic (cleaved caspase 3+) cardiomyocytes. The ultrastructural examination provided further details on the degenerative processes. Randomly distributed cardiomyocytes exhibited swollen mitochondria (Fig. 29), accumulations of membrane-bound multivesicular bodies and lamellar bodies, a complete loss of organelles, and/or an accumulation of fluid and electron-dense debris within the sarcoplasm (Figs. 30, 31). Cardiomyocytes sometimes exhibited irregularly thickened and electron-dense Z disks, and occasionally disruption of the intercalated discs. In addition, there were occasional cardiomyocytes that showed a substantially enlarged nucleus with finely dispersed chromatin (Figs. 32, 33), suggesting hypertrophy of the cell.[98]
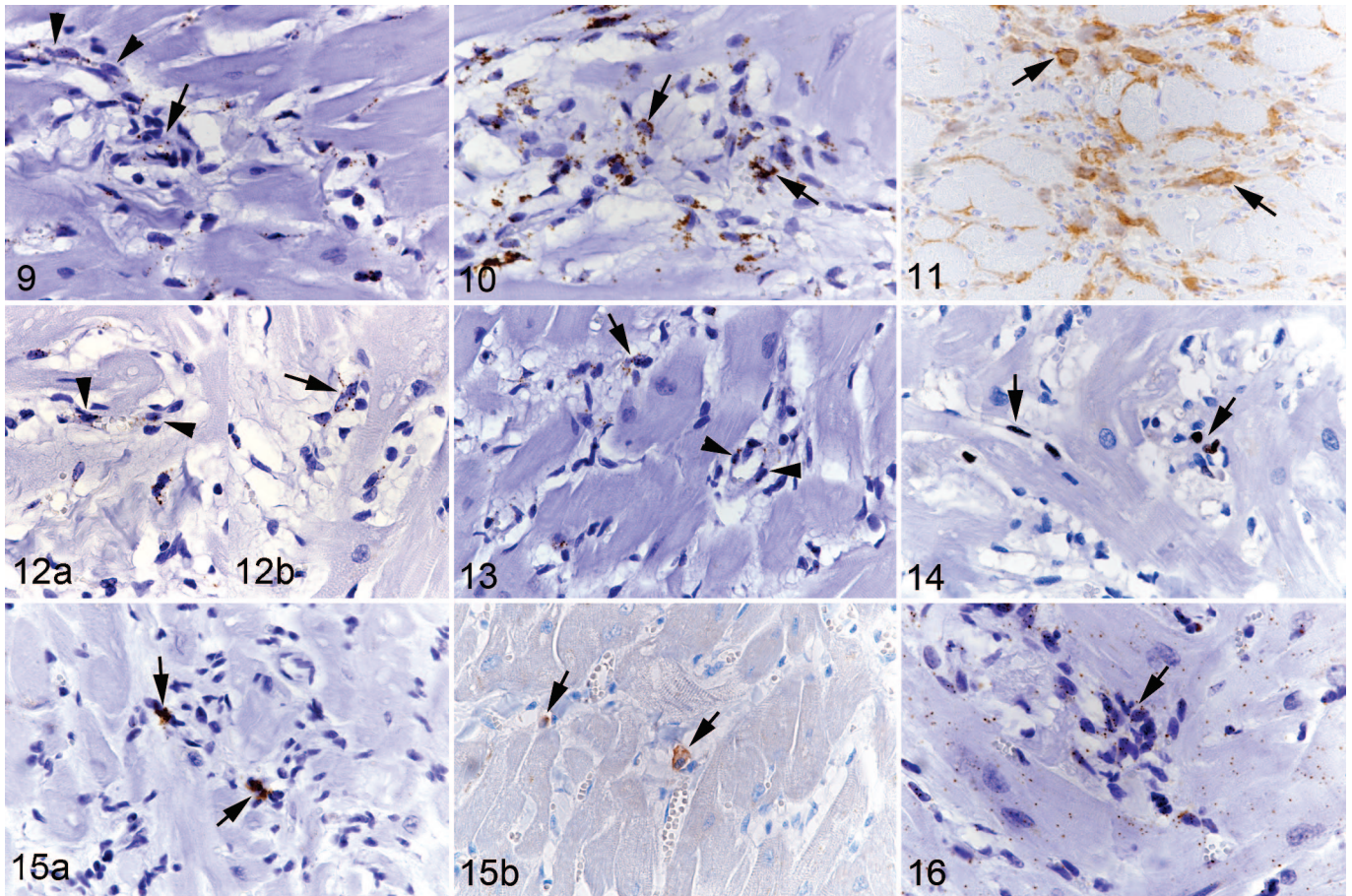
Figures 9–16. Hypertrophic cardiomyopathy, left ventricular free wall, cat. **Figure 9.** Case 11. CD34 mRNA expression is seen in the cytoplasm of capillary endothelial cells (arrowheads) and a large proportion of interstitial cells, some of which are arranged in rudimentary ring-shaped structures reminiscent of primitive vessels (arrow). RNA-in situ hybridization (RNA-ISH). **Figure 10.** Case 8. A large proportion of interstitial cells express Col1A1 mRNA the cytoplasm (arrows). RNA-ISH. **Figure 11.** Case 13. A moderate number of interstitial cells are positive for procollagen I protein (arrows). Immunohistochemistry (IHC). **Figure 12.** Case 11. VEGFR2 mRNA expression is seen in the cytoplasm of capillary endothelial cells (arrowheads; [a]), and in several interstitial cells some of which are arranged in rudimentary ring-shaped structures reminiscent of primitive vessels (arrow; [b]). RNA-ISH. **Figure 13.** Case 11. PDGFRB mRNA expression is seen in the cytoplasm of cells surrounding capillary endothelial cells (pericytes; arrowheads), and in several interstitial cells some of which are arranged in rudimentary ring-shaped structures reminiscent of primitive vessels (arrow). RNA-ISH. **Figure 14.** Case 8. A few round and spindle-shaped cells in the interstitium express the proliferation marker Ki67 in the nucleus (arrows). IHC. **Figure 15.** Case 8. (a) Scattered individual cells in the interstitium express Kit mRNA in the cytoplasm and nucleus (arrows). RNA-ISH. (b) Rare interstitial cells show Kit protein expression (arrows). IHC. **Figure 16.** Case 8. Almost all interstitial cells show a positive signal for MEF2C mRNA in the cytoplasm (arrow). This is also seen in cardiomyocytes. RNA-ISH.

In all HCM cases, cardiomyocytes exhibited moderate MEF2C mRNA signals (Fig. 33), whereas a weak MEF2C signal was generally seen in the cardiomyocytes of the control hearts (Suppl. Fig. S11). CD29 transcription was consistently observed in cardiomyocytes both in control and HCM cats. However, while the signal was generally weak in control animals (Suppl. Fig. S12), it was strong in HCM, where individual cells in areas with more severe interstitial widening due to fibrosis and/or edema showed a signal of even higher intensity (Fig. 34). In 5 cats (cases 1, 3, 6, 10, and 11), a small number of cardiomyocytes was also found to transcribe Kit; the signal was of moderate intensity and observed in the perinuclear cytoplasm and/or in the nucleus (Fig. 35). Immunohistology confirmed Kit protein expression in individual cardiomyocytes

(Fig. 36), although in fewer cells than those with an mRNA signal. There was no evidence of an association between Kit expression and degenerative changes. One control animal (case C4) also exhibited scattered cardiomyocytes with a moderate Kit mRNA signal in the perinuclear sarcoplasm, without any apparent morphological change (Suppl. Fig. S13); Kit protein was not expressed.

Discussion

The present study is a follow-up of our recently published work which showed that fHCM is associated with myocardial remodeling in a pro-inflammatory environment.[50] It suggested that macrophages and the vasculature play important roles in the
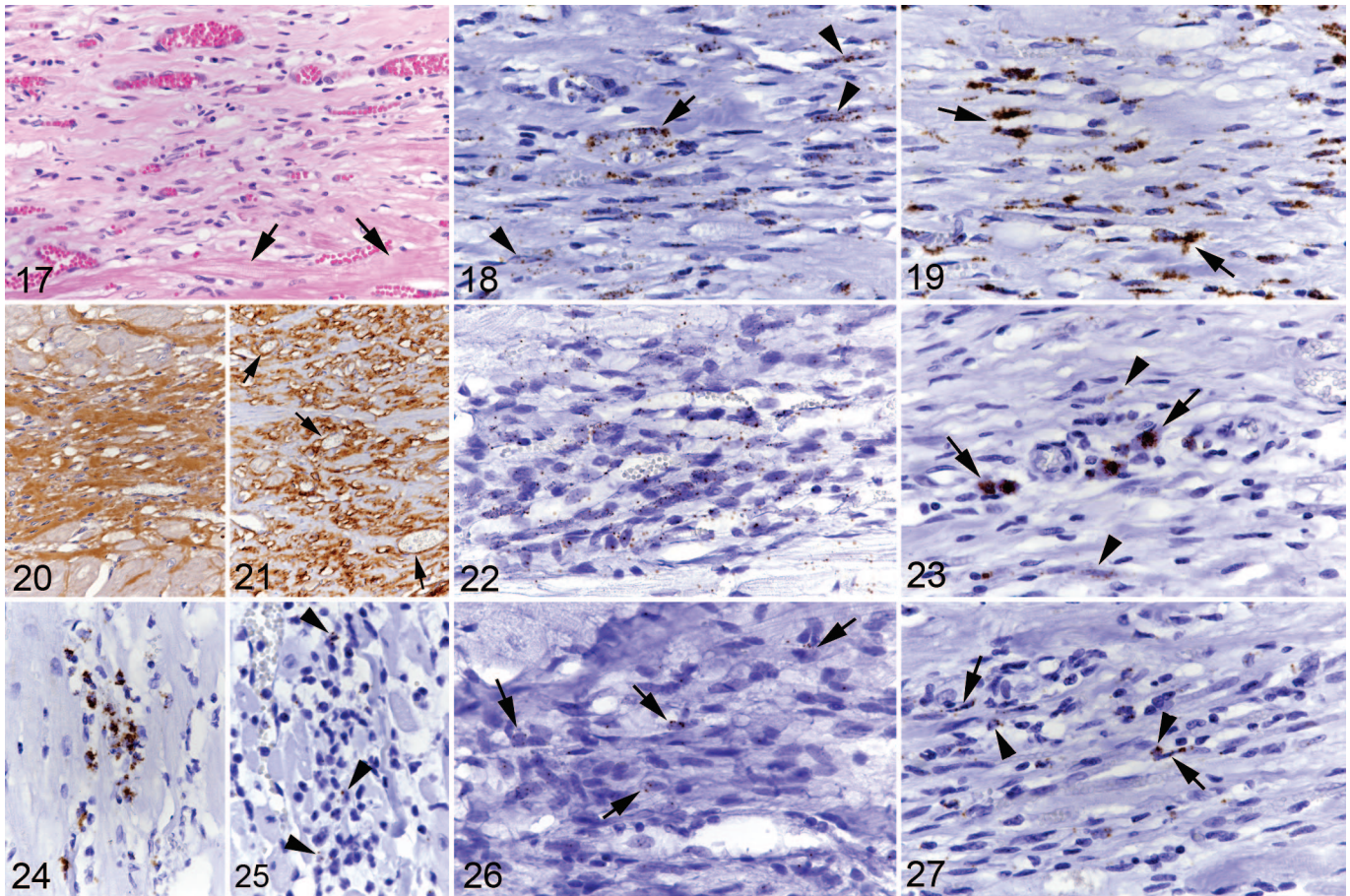
Figures 17–27. Hypertrophic cardiomyopathy, left ventricular free wall, cat. Focal area of cell-rich fibrosis with abundant small and medium-sized vessels. **Figure 17.** Case 1. Focal area of cell- and vessel-rich fibrous connective tissue. Arrows: adjacent cardiomyocytes. Hematoxylin eosin (HE). **Figure 18.** Case 1. Numerous, predominantly spindle-shaped cells (arrowheads) as well as vascular endothelial cells (arrow) express CD34 mRNA. RNA-in situ hybridization (RNA-ISH). **Figure 19.** Case 1. There are numerous, mainly spindle-shaped cells with strong Col1A1 mRNA signal (arrows). RNA-ISH. **Figure 20.** Case 12. Area with lower cellularity exhibiting abundant collagen I deposition. Immunohistochemistry (IHC). **Figure 21.** Case 12. Collagen IV deposition is predominantly seen around vessels (arrows). IHC. **Figure 22.** Case 12. The majority of cells within the focal lesion exhibit a weak MEF2C mRNA signal. RNA-ISH. **Figure 23.** Case 1. Focal lesion with a few individual Kit mRNA positive round cells consistent with mast cells (arrows) and rare elongate cells with a weak signal (arrowheads). RNA-ISH. **Figure 24.** Case 1. Small cluster of CD14 mRNA positive round cells in the interstitium. RNA-ISH. **Figure 25.** Case 10. Rare individual round cells in the interstitium exhibit a weak CCR2 signal (arrowheads). RNA-ISH. **Figure 26.** Case 12. Several elongate to spindle-shaped cells in a focal area of cell-rich fibrosis exhibit a weak CD14 signal (arrows). RNA-ISH. **Figure 27.** Case 1. Several round cells (arrowheads) and spindle-shaped cells (arrows) in a focal area of cell-rich fibrosis exhibit a weak CCR2 signal. RNA-ISH.

pathogenesis of fHCM, providing evidence that ischemic processes are underlying the pathological changes and eventually lead to multifocal infarct-like lesions.[50] In human HCM, similar remodeling processes take place; however, these are accompanied by microvascular dysfunction and a reduced capillary density,[15,33,40,53,55,83] and they seem to trigger an increase in circulating stem cells.[41,65] The present study aimed to provide further insights into the nature of the pathogenetic processes in fHCM; based on our previous findings and analogous to human HCM, it focused on structural changes in the myocardial microvasculature and the involvement of cardiac and blood-derived stem cell and progenitor cell populations.

Our results confirm that in fHCM the interstitium undergoes substantial structural changes. The most obvious was a significantly reduced capillary density (ie, lower number of capillaries per cross-sectional myocardial area) and a relative increase of the space occupied by the interstitium (ie, higher proportion of tissue occupied by interstitial edema and/or collagen per cross-sectional myocardial area) in fHCM compared to control animals. This suggests that the reduced capillary density is the consequence of an interstitial widening due to edema and collagen deposition.[33]

We found that the capillaries were often irregularly arranged. While they were aligned in parallel to cardiomyocytes in the unaltered myocardium, they were bent or twisted and formed branches in HCM. Ultrastructural examination confirmed these findings and also revealed irregularities in the capillary walls, with evidence of endothelial cell degeneration (endothelial cell
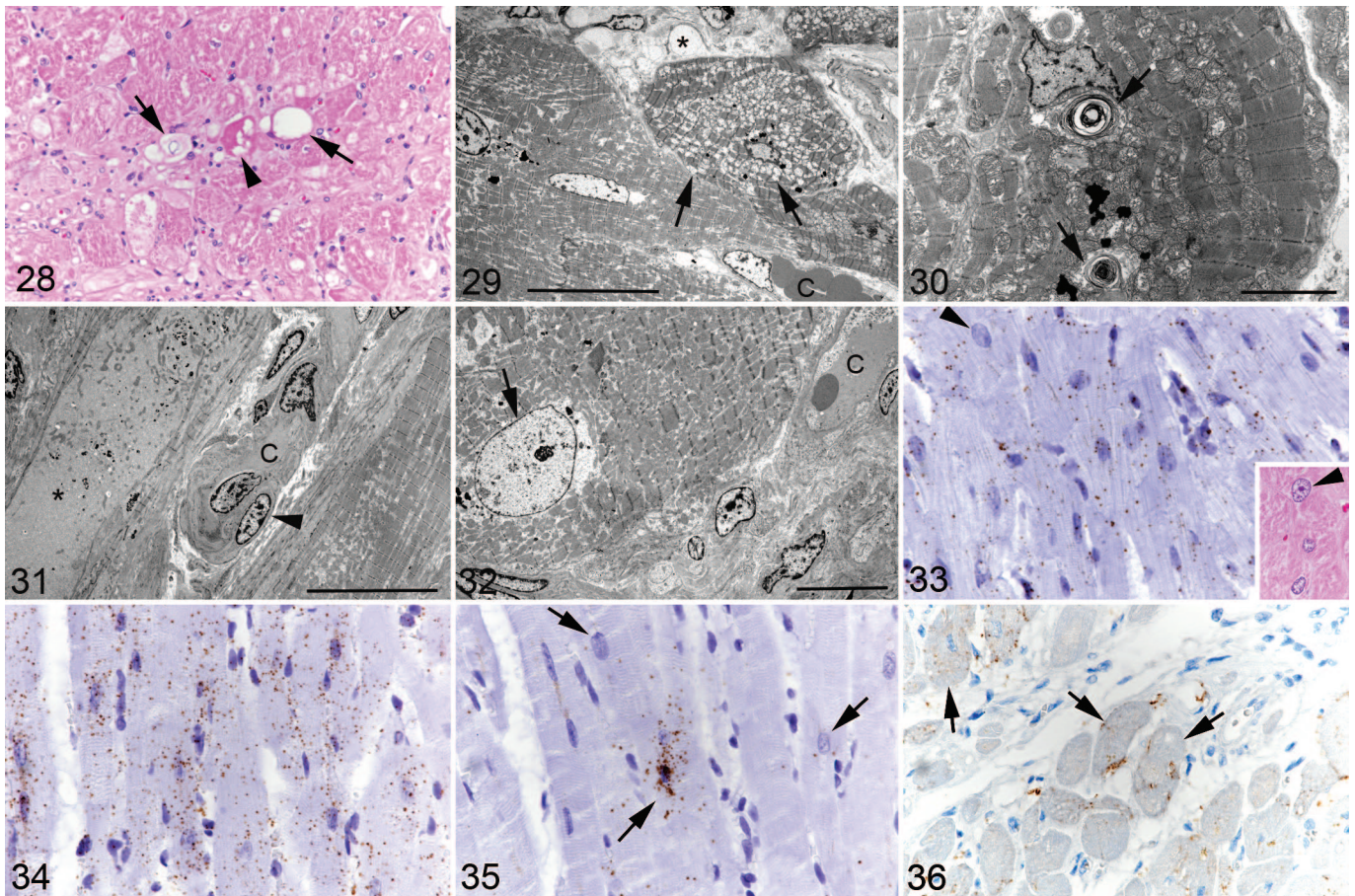
Figures 28–36. Hypertrophic cardiomyopathy, left ventricular free wall, cat. **Figure 28.** Case 13. Individual degenerating cardiomyocytes showing sarcoplasmic vacuolation (arrows), hypereosinophilia, and vacuolated and hypereosinophilic sarcoplasm (arrowhead). Hematoxylin eosin (HE). **Figure 29.** Case 12. Degenerating cardiomyocyte. Mitochondria exhibit diffuse swelling (arrows). C: interstitial capillary. Asterisk: interstitial edema. Transmission electron microscopy (TEM); bar = 20 µm. **Figure 30.** Case 16. Cardiomyocytes with cytoplasmic lamellar bodies (arrows). TEM; bar = 5 µm. **Figure 31.** Case 13. Degenerate cardiomyocyte (asterisk) with loss of organelles. The cytoplasm contains fluid and electron-dense debris. C: interstitial capillary with plump endothelial cells and irregular basement membrane. Arrowhead: pericyte. TEM; bar = 20 µm. **Figure 32.** Case 13. Cardiomyocyte with enlarged nucleus with finely dispersed chromatin (arrow). C: interstitial capillary. TEM; bar = 10 µm. **Figure 33.** Case 5. Cardiomyocytes exhibit moderate MEF2C mRNA signals. Individual cardiomyocytes exhibit an enlarged nucleus (arrowhead). RNA-ISH. Inset: consecutive section, showing a cardiomyocyte with an enlarged nucleus (arrowhead). **Figure 34.** Case 5. Cardiomyocytes exhibit strong CD29 mRNA signals. RNA-ISH. **Figure 35.** Case 5. Cardiomyocytes exhibit a variable Kit mRNA signal (arrows). RNA-ISH. **Figure 36.** Case 5. Several cardiomyocytes show Kit protein expression (arrows). Immunohistochemistry.

swelling) and activation (enlarged nucleus), the presence of enlarged reactive pericytes, and thickening of the basement membrane. These findings suggest that the interstitial remodeling processes in fHCM could develop from structural changes in the myocardial capillary bed that lead to increased capillary leakage and interstitial edema, resulting in widening of intercellular spaces and thereby an increased diffusion distance which would render the cardiomyocytes prone to ischemia. What triggers the vascular changes in the first place is not yet known, but the apparent subsequent increased permeability and edema could set off the more obvious remodeling processes such as collagen deposition. The concept of myocardial interstitial edema is not entirely new in cats. It has been suspected as the process underlying a transient myocardial thickening observed in cats that presented with clinical findings consistent with HCM which later resolved.[75] Thickening of the ventricular wall due to interstitial edema instead of "real" hypertrophy could also explain, at least in part, the lack of clear evidence of cardiomyocyte hypertrophy in fHCM. Two studies have so far attempted quantification of cardiomyocyte size; they did not find a correlation between the increase in cardiac thickening and cardiomyocyte diameter.[44,50] However, our findings suggest that cardiomyocytes at least attempt to become hypertrophic which could indicate the optimal technical approach to assess the parameters has yet to be taken.

Beside the preexisting differentiated vessels, the interstitium also harbored variable numbers of individual spindle-shaped to slightly plumper cells that expressed VEGFR2,

PDGFRB, and/or CD34 mRNA. Expression of VEGFR2, the main receptor of the VEGF family, identifies a proportion of the cells as endothelial cells, and indeed we also found that VEGFR2 was expressed by endothelial cells of differentiated capillaries.[91] On the other hand, expression of PDGFRB indicates that other cells are pericytes and/or vascular smooth muscle cells, in line also with its transcription by cells around capillaries.[43] The transcription of CD34 suggests that a proportion of cells could have progenitor cell capabilities.[38,74,90] However, previous studies in cats have shown CD34 expression in endothelial cells which we also observed in differentiated capillaries.[39,72] We found VEGFR2, PDGFRB, and CD34 mRNA positive interstitial cells arranged in ring-shaped structures that resembled primitive blood vessels; this would suggest attempts at angiogenesis. In particular the transcription of CD34 could indicate some degree of stemness of these cells, and their involvement in vascular homeostasis.[90] In human patients, HCM was found to be associated with an increase in CD45−/CD34+/VEGFR2+ and CD45−/CD34+/CD133+ circulating endothelial progenitor cells (EPC) which was hypothesized to play a role in angiogenic processes in the myocardium.[41] While we found interstitial cells with strong CD34 transcription and cells with a VEGFR2 mRNA signal, there were none transcribing CD133. Since CD133 is rapidly lost with differentiation of EPCs and immature endothelial cells and is generally expressed in stem cells,[34,78] the absence of cells transcribing CD133 could indicate that the progenitor cells involved in the remodeling processes in fHCM are generally in a more advanced stage of differentiation.

Overall, in HCM hearts we observed substantially more CD34 than VEGFR2 and PDGFRB mRNA positive cells in the interstitium. This suggests that CD34 transcription was not limited to cells of vascular phenotype. In both mice and man, CD34 can be expressed in mesenchymal stem cells (MSC), and in mice, CD34+ MSCs were shown to have enhanced proliferative and angiogenic capacity compared to CD34− MSC.[19,66] Also, in humans, CD34+ fibrocytes have been described in multiple organs.[10] Hence, a proportion of the CD34+ cells in the interstitium of the fHCM hearts could represent non-endothelial mesenchymal populations, and in particular fibroblasts. Indeed, the large proportion of fibroblasts in the interstitium, as identified based on their Col1A1 transcription,[42] supports this interpretation and even suggests CD34 and Col1A1 co-expression in a proportion of cells. Alongside this, the morphometric analyses identified a significantly higher amount of interstitial collagen in HCM than in control hearts, which immunohistochemistry confirmed to be mainly collagen I. When activated (ie, after tissue damage or during remodeling processes), fibroblasts differentiate into myofibroblasts and transcribe the ACTA2 gene which encodes αSMA.[94] This could explain our previous observation of a significant increase in αSMA positive cells in the interstitium of fHCM hearts.[50] At the time we considered these as evidence of an increase in small- to medium-sized vessels which, in light of the present findings, was apparently a misinterpretation. We also found a small number of interstitial cells that transcribed MEF2C, a cardiogenic transcription factor.[3] It is known that the phenotype of fibroblasts depends on their tissue environment; for example, in mice, MEF2C was found to be transcribed in cardiac fibroblasts. This indicates that the MEF2C mRNA positive cells in fHCM also represent subsets of fibroblasts.[31]

Interestingly, we also observed individual Kit mRNA positive cells which could represent subpopulations of stem cells.[64] On the other hand, the complete lack of Nanog and Octa4 mRNA expression allows us to rule out the option of stem cell pluripotency.[101,102] Alternatively, the Kit mRNA positive cells could represent the so-called telocytes, which are Cajal-like cells that have been described in human and murine hearts.[52] Telocytes co-express Kit, CD34, and PDGFRB and seem to play an active role in the progression of cardiac interstitial remodeling.[52] However, since telocytes have not been described in cats, further studies are required to determine their existence and potential role in this species.

Labeling for Ki67 revealed that a small proportion of interstitial cells was proliferating, these were spindle-shaped cells, round cells with macrophage morphology, and occasional capillary endothelial cells. This finding indicates that the interstitial remodeling processes in fHCM involve the local proliferation of these cell populations.

In order to gain some basic mechanistic insight into the processes underlying fHCM we assessed the transcription of CD29 (integrin subunit beta 1) since integrins including CD29 are known to also play a role in cardiac remodeling, as they facilitate the progression of cardiac fibrosis by mediating the differentiation of fibroblasts into myofibroblasts.[18] Indeed, we observed CD29 transcription in all interstitial cells and in cardiomyocytes in HCM, whereas the signal was present but consistently weak in control hearts. The apparently substantial CD29 upregulation in fHCM would be consistent with a role of this integrin in the pathogenic processes in fHCM, providing evidence of an intense crosstalk between interstitial cells themselves and with cardiomyocytes which we also found to express CD29 mRNA.

As previously described, fHCM is associated with a significant increase in interstitial Iba1-positive macrophages.[50] We know from humans and mice that the normal myocardial macrophage population is heterogeneous and consists of both resident macrophages and blood-derived macrophages.[22,36] Since Iba1 is a pan-macrophage marker that cannot discern between monocytes and macrophages at different stages of differentiation,[51] we made a first attempt at dissecting the macrophage populations in the feline heart by addressing their direct monocyte origin. The quantification of cells expressing calprotectin, a marker of monocytes and recently blood-derived macrophages,[47,92] confirmed the presence of the latter in both the control and HCM myocardium. Their number was higher in HCM; however, their proportion in relation to the overall macrophage population (Iba1+) was lower in HCM compared to control animals, though the difference was not significant. Considering the concurrent increase in Ki67 positive cells with macrophage morphology in the interstitium in HCM, proliferation of resident macrophages is indeed likely. We also assessed the transcription of CD14 and CCR2, in the attempt to further classify

the macrophages according to their counterparts in humans (Table 1). In humans, circulating monocytes are classified into 3 subtypes, two with pro-inflammatory functions, the so-called classical (CD14++, CD16−, and CCR2++) and intermediate (CD14++, CD16+, and CCR2+) monocytes, and a third known as nonclassical (CD14+, CD16++, and CCR2−) monocytes which have anti-inflammatory functions.[27] The human and murine heart contains both CCR2+ and CCR2− macrophages. These have different origin and functions: while CCR2− macrophages are of embryonic origin and tend to play regenerative roles, CCR2+ macrophages are monocyte-derived and promote inflammatory responses (Table 1).[36] The current study identified scattered individual CD14 and/or CCR2 mRNA positive cells among the mononuclear cells in the interstitium. We observed only rare monocytes with a weak signal for either marker (data not shown). Together with the fact that CD14 expression has been observed in only a small proportion of bone marrow cells and was variable in peripheral blood monocytes of healthy cats,[5,99] this raises the question of how confidently we can extrapolate markers of the different monocyte phenotypes from humans to cats. Our findings show that fHCM is not dominated by cells that transcribe CD14 or CCR2; however, this does not necessarily allow us to draw conclusions with regards to the protein expression of these markers.[57] Nonetheless, our findings provide further evidence of the heterogeneous nature of macrophage populations also in cats and highlight the necessity of further investigations into feline intracardiac macrophage populations, their origin and local proliferation in fHCM.

We have previously shown that fHCM is associated with focal areas of cardiomyocyte replacement by cell-rich fibrosis with abundant vessels. These areas resemble chronic infarcts and could therefore be the result of ischemic events.[50] Such focal lesions were also seen in a proportion of cases in the present cohort. The focal lesions and the interstitial processes have a similar composition which suggests that they represent a focal exacerbation of the interstitial processes. Besides mature blood vessels (CD31+), fibroblasts (Col1A1+) and macrophages (Iba1+, occasional calprotectin-positive and CD14/CCR2 mRNA-positive cells), they contained CD34 mRNA positive spindle-shaped cells and cells with a vascular phenotype (VEGFR2/PDGFR2 mRNA positive). Also, the presence of scattered spindle-shaped fibroblast-like cells that showed a CD14, MEF2C, and/or Kit mRNA signal in some cases provides further evidence of the potential plasticity of this cell population. Further support toward this comes from in vitro studies that have identified human CD14+ cells with progenitor cell capacity that co-expressed myeloid, vascular and fibroblast markers.[54,89] Interestingly, the focal lesions generally contained at least a few Kit-positive mast cells. Mast cells have also been found in human cardiovascular disease, where they seem to play a role in the exacerbation of fibrotic lesions.[58] Further investigations are needed to identify their role in fHCM.

In line with a potential ischemic basis for the myocardial lesions of fHCM, cardiomyocytes were found to exhibit subtle degenerative changes typically seen with hypoxia, such as swollen mitochondria and evidence of fluid accumulation. Also, apoptotic cardiomyocytes were very rare, whereas there were a few cells with more overt damage, such as thickening of the Z disks, disruption of the intercalated discs, loss of striation, and necrosis, all compatible with cell death due to hypoxia and energy deprivation.[17,50] The structural changes were seen alongside some phenotypic alterations in morphologically unaltered cardiomyocytes. We found evidence of substantial CD29 mRNA upregulation in cardiomyocytes, a feature shown to occur under conditions of cell stress that is linked with the activation of pro-survival pathways, hence representing a cellular defense mechanism.[85] On the other hand, in murine studies it has been hypothesized that mechanical signals in the cardiomyocyte could trigger an integrin response that activates hypertrophic signaling pathways.[18]

Interestingly, we also found evidence of mild upregulation of MEF2C transcription. MEF2C is a cardiogenic transcription factor which, in adult human hearts, is also involved in transcriptional regulation processes associated with pathological cardiac hypertrophy.[3,4] We also found random, otherwise morphologically unaltered cardiomyocytes with enlarged vesicular nuclei; these could be indicative of activation and attempts at hypertrophy.[32] Finally, we also observed consistent expression of both Kit mRNA and protein in a variable proportion of cardiomyocytes. It is known that cardiomyocytes can express Kit; however, why they do this and what is its exact physiological role in cardiomyocytes is still not clear.[21,60] Overall, our results indicate that in fHCM cardiomyocytes undergo phenotypical changes that might aim to secure the cell's survival and hypertrophy, likely as a compensatory mechanism. Whether these efforts do indeed lead to cardiomyocyte hypertrophy requires further investigations, optimally using 3D imaging techniques. In addition, further assessment of structural alterations in combination with molecular signaling pathways would be equally useful.

The present study has some limitations. The age of the control group did not match that of the HCM cats, as it was mainly composed of animals of 1.5 years of age; however, our previous study did not find age-related differences in collagen deposition, interstitial widening, and the ratio of contractile versus noncontractile tissue in feline hearts.[50] In our opinion, this is likely also applicable to the capillary density. The morphometric approach to assess the capillary density was based on the quantification of capillary profiles per unit area in one transverse histological section. This approach might introduce some bias as it lacks an unbiased random sampling.[71] Finally, single marker approaches limit the options for the identification of specific cell phenotypes. Using the RNA-ISH approach which we chose to overcome the lack of antibodies that reliably detect the markers of interest in feline tissue, however, excluded double or triple staining. Nonetheless, the present study sets the ground for future more specific studies. In particular, the CD34+ populations, their progenitor cell properties, and their involvement in the progression of fHCM should be further investigated. Also, the intracardiac macrophage populations

need to be better characterized to understand the pathophysiology of the disease. Finally, microvascular structural alterations should be further investigated for their association with myocardial ischemia.

ORCID iD

Anja Kipar (iD) https://orcid.org/0000-0001-7289-3459

References

1. Abbott JA. Feline hypertrophic cardiomyopathy: an update. *Vet Clin North Am Small Anim Pract*. 2010;**40**(4):685–700.
2. Adams RH, Alitalo K. Molecular regulation of angiogenesis and lymphangiogenesis. *Nat Rev Mol Cell Biol*. 2007;**8**(6):464–478.
3. Akazawa H, Komuro I. Roles of cardiac transcription factors in cardiac hypertrophy. *Circ Res*. 2003;**92**(10):1079–1088.
4. Alonso-Montes C, Naves-Diaz M, Fernandez-Martin JL, et al. New polymorphisms in human MEF2C gene as potential modifier of hypertrophic cardiomyopathy. *Mol Biol Rep*. 2012;**39**(9):8777–8785.
5. Araghi A, Nassiri SM, Atyabi N, et al. Flow cytometric immunophenotyping of feline bone marrow cells and haematopoietic progenitor cells using anti-human antibodies. *J Feline Med Surg*. 2014;**16**(4):265–274.
6. Atkins CE, Gallo AM, Kurzman ID, et al. Risk factors, clinical signs, and survival in cats with a clinical diagnosis of idiopathic hypertrophic cardiomyopathy: 74 cases (1985–1989). *J Am Vet Med Assoc*. 1992;**201**(4):613–618.
7. Avolio E, Madeddu P. Discovering cardiac pericyte biology: from physiopathological mechanisms to potential therapeutic applications in ischemic heart disease. *Vascul Pharmacol*. 2016;**86**:53–63.
8. Bajpai G, Bredemeyer A, Li W, et al. Tissue resident CCR2− and CCR2+ cardiac macrophages differentially orchestrate monocyte recruitment and fate specification following myocardial injury. *Circ Res*. 2019;**124**(2):263–278.
9. Bajpai G, Schneider C, Wong N, et al. The human heart contains distinct macrophage subsets with divergent origins and functions. *Nat Med*. 2018;**24**(8):1234–1245.
10. Barth PJ, Westhoff CC. CD34+ fibrocytes: morphology, histogenesis and function. *Curr Stem Cell Res Ther*. 2007;**2**(3):221–227.
11. Barzegar Behrooz A, Syahir A, Ahmad S. CD133: beyond a cancer stem cell biomarker. *J Drug Target*. 2019;**27**(3):257–269.
12. Biasato I, Francescone L, La Rosa G, et al. Anatomopathological staging of feline hypertrophic cardiomyopathy through quantitative evaluation based on morphometric and histopathological data. *Res Vet Sci*. 2015;**102**:136–141.
13. Bonsembiante F, Benali SL, Trez D, et al. Histological and immunohistochemical characterization of feline renal cell carcinoma: a case series. *J Vet Med Sci*. 2016;**78**(6):1039–1043.
14. Brólio MP, Vidane AS, Zomer HD, et al. Morphological characterization of the progenitor blood cells in canine and feline umbilical cord. *Microsc Res Tech*. 2012;**75**(6):766–770.
15. Cecchi F, Sgalambro A, Baldi M, et al. Microvascular dysfunction, myocardial ischemia, and progression to heart failure in patients with hypertrophic cardiomyopathy. *J Cardiovasc Transl Res*. 2009;**2**(4):452–461.
16. Chen X, Gao B, Ponnusamy M, et al. MEF2 signaling and human diseases. *Oncotarget*. 2017;**8**(67):112152–112165.
17. Christiansen LB, Prats C, Hyttel P, et al. Ultrastructural myocardial changes in seven cats with spontaneous hypertrophic cardiomyopathy. *J Vet Cardiol*. 2015;**17**(suppl 1):S220–S232.
18. Civitarese RA, Kapus A, McCulloch CA, et al. Role of integrins in mediating cardiac fibroblast-cardiomyocyte cross talk: a dynamic relationship in cardiac biology and pathophysiology. *Basic Res Cardiol*. 2017;**112**(1):6.
19. Copland I, Sharma K, Lejeune L, et al. CD34 expression on murine marrow-derived mesenchymal stromal cells: impact on neovascularization. *Exp Hematol*. 2008;**36**(1):93–103.
20. Dutton LC, Dudhia J, Guest DJ, et al. Inducing pluripotency in the domestic cat (*Felis catus*). *Stem Cells Dev*. 2019;**28**(19):1299–1309.
21. Ellison GM, Vicinanza C, Smith AJ, et al. Adult c-kit(pos) cardiac stem cells are necessary and sufficient for functional cardiac regeneration and repair. *Cell*. 2013;**154**(4):827–842.
22. Epelman S, Lavine KJ, Beaudin AE, et al. Embryonic and adult-derived resident cardiac macrophages are maintained through distinct mechanisms at steady state and during inflammation. *Immunity*. 2014;**40**(1):91–104.
23. Ferasin L. Feline myocardial disease. 1: classification, pathophysiology and clinical presentation. *J Feline Med Surg*. 2009;**11**(1):3–13.
24. Fox PR.Hypertrophic cardiomyopathy. Clinical and pathologic correlates. *J Vet Cardiol*. 2003;**5**(2):39–45.
25. Fox PR, Keene BW, Lamb K, et al. International collaborative study to assess cardiovascular risk and evaluate long-term health in cats with preclinical hypertrophic cardiomyopathy and apparently healthy cats: the reveal study. *J Vet Intern Med*. 2018;**32**(3):930–943.
26. Fox PR, Liu SK, Maron BJ. Echocardiographic assessment of spontaneously occurring feline hypertrophic cardiomyopathy. An animal model of human disease. *Circulation*. 1995;**92**(9):2645–2651.
27. Franca CN, Izar MCO, Hortencio MNS, et al. Monocyte subtypes and the CCR2 chemokine receptor in cardiovascular disease. *Clin Sci (Lond)*. 2017;**131**(12):1215–1224.
28. Freer G, Matteucci D, Mazzetti P, et al. Generation of feline dendritic cells derived from peripheral blood monocytes for in vivo use. *Clin Diagn Lab Immunol*. 2005;**12**(10):1202–1208.
29. Frey N, Luedde M, Katus HA. Mechanisms of disease: hypertrophic cardiomyopathy. *Nat Rev Cardiol*. 2011;**9**(2):91–100.
30. Fuentes T, Kearns-Jonker M. Endogenous cardiac stem cells for the treatment of heart failure. *Stem Cells Cloning*. 2013;**6**:1–12.
31. Furtado MB, Costa MW, Pranoto EA, et al. Cardiogenic genes expressed in cardiac fibroblasts contribute to heart development and repair. *Circ Res*. 2014;**114**(9):1422–1434.
32. Gerdes AM, Liu Z, Zimmer HG. Changes in nuclear size of cardiac myocytes during the development and progression of hypertrophy in rats. *Cardioscience*. 1994;**5**(3):203–208.
33. Güçlü A, Happé C, Eren S, et al. Left ventricular outflow tract gradient is associated with reduced capillary density in hypertrophic cardiomyopathy irrespective of genotype. *Eur J Clin Invest*. 2015;**45**(12):1252–1259.
34. Handgretinger R, Kuçi S. CD133-positive hematopoietic stem cells: from biology to medicine. In: Corbeil D, ed. *Prominin-1 (CD133): New Insights on Stem & Cancer Stem Cell Biology*. Springer; 2013:99–111.

35. Hesse M, Fleischmann BK, Kotlikoff MI. Concise review: the role of C-kit expressing cells in heart repair at the neonatal and adult stage. *Stem Cells*. 2014;**32**(7):1701–1712.

36. Hulsmans M, Sam F, Nahrendorf M. Monocyte and macrophage contributions to cardiac remodeling. *J Mol Cell Cardiol*. 2016;**93**:149–155.

37. Ironside VA, Tricklebank PR, Boswood A. Risk indictors in cats with preclinical hypertrophic cardiomyopathy: a prospective cohort study. *J Feline Med Surg*. 2020;**23**(2):149–159.

38. Ivanovic Z. Hematopoietic stem cells in research and clinical applications: the "CD34 issue." *World J Stem Cells*. 2010;**2**(2):18–23.

39. Jennings RN, Miller MA, Ramos-Vara JA. Comparison of CD34, CD31, and factor VIII-related antigen immunohistochemical expression in feline vascular neoplasms and CD34 expression in feline nonvascular neoplasms. *Vet Pathol*. 2012;**49**(3):532–537.

40. Johansson B, Morner S, Waldenstrom A, et al. Myocardial capillary supply is limited in hypertrophic cardiomyopathy: a morphological analysis. *Int J Cardiol*. 2008;**126**(2):252–257.

41. Kalyva A, Marketou ME, Parthenakis FI, et al. Endothelial progenitor cells as markers of severity in hypertrophic cardiomyopathy. *Eur J Heart Fail*. 2016;**18**(2):179–184.

42. Karsenty G, Park RW. Regulation of type I collagen genes expression. *Int Rev Immunol*. 1995;**12**(2–4):177–185.

43. Kazlauskas A. PDGFs and their receptors. *Gene*. 2017;**614**:1–7.

44. Kershaw O, Heblinski N, Lotz F, et al. Diagnostic value of morphometry in feline hypertrophic cardiomyopathy. *J Comp Pathol*. 2012;**147**(1):73–83.

45. Khor KH, Campbell FE, Owen H, et al. Myocardial collagen deposition and inflammatory cell infiltration in cats with pre-clinical hypertrophic cardiomyopathy. *Vet J*. 2015;**203**(2):161–168.

46. Kim HR, Lee J, Byeon JS, et al. Extensive characterization of feline intra-abdominal adipose-derived mesenchymal stem cells. *J Vet Sci*. 2017;**18**(3):299–306.

47. Kipar A, Bellmann S, Kremendahl J, et al. Cellular composition, coronavirus antigen expression and production of specific antibodies in lesions in feline infectious peritonitis. *Vet Immunol Immunopathol*. 1998;**65**(2–4):243–257.

48. Kittleson MD, Meurs KM, Harris SP. The genetic basis of hypertrophic cardiomyopathy in cats and humans. *J Vet Cardiol*. 2015;**17**(suppl 1):S53–S73.

49. Kittleson MD, Meurs KM, Munro MJ, et al. Familial hypertrophic cardiomyopathy in Maine Coon cats: an animal model of human disease. *Circulation*. 1999;**99**(24):3172–3180.

50. Kitz S, Fonfara S, Hahn S, et al. Feline hypertrophic cardiomyopathy: the consequence of cardiomyocyte-initiated and macrophage-driven remodeling processes? *Vet Pathol*. 2019;**56**(4):565–575.

51. Köhler C. Allograft inflammatory factor-1/Ionized calcium-binding adapter molecule 1 is specifically expressed by most subpopulations of macrophages and spermatids in testis. *Cell Tissue Res*. 2007;**330**(2):291–302.

52. Kostin S. Cardiac telocytes in normal and diseased hearts. *Semin Cell Dev Biol*. 2016;**55**:22–30.

53. Kuusisto J, Karja V, Sipola P, et al. Low-grade inflammation and the phenotypic expression of myocardial fibrosis in hypertrophic cardiomyopathy. *Heart*. 2012;**98**(13):1007–1013.

54. Kuwana M, Okazaki Y, Kodama H, et al. Human circulating CD14+ monocytes as a source of progenitors that exhibit mesenchymal cell differentiation. *J Leukoc Biol*. 2003;**74**(5):833–845.

55. Lamke GT, Allen RD, Edwards WD, et al. Surgical pathology of subaortic septal myectomy associated with hypertrophic cardiomyopathy. A study of 204 cases (1996–2000). *Cardiovasc Pathol*. 2003;**12**(3):149–158.

56. Lawson JS, Syme HM, Wheeler-Jones CPD, et al. Characterisation of feline renal cortical fibroblast cultures and their transcriptional response to transforming growth factor β1. *BMC Vet Res*. 2018;**14**(1):76.

57. Leuschner F, Nahrendorf M. Novel functions of macrophages in the heart: insights into electrical conduction, stress, and diastolic dysfunction. *Eur Heart J*. 2020;**41**(9):989–994.

58. Levick SP, Melendez GC, Plante E, et al. Cardiac mast cells: the centrepiece in adverse myocardial remodelling. *Cardiovasc Res*. 2011;**89**(1):12–19.

59. Li S, Guo K, Wu J, et al. Altered expression of c-kit and nanog in a rat model of Adriamycin-induced chronic heart failure. *Am J Cardiovasc Dis*. 2017;**7**(2):57–63.

60. Liu Q, Yang R, Huang X, et al. Genetic lineage tracing identifies in situ Kit-expressing cardiomyocytes. *Cell Res*. 2016;**26**(1):119–130.

61. Luis Fuentes V, Abbott J, Chetboul V, et al. ACVIM consensus statement guidelines for the classification, diagnosis, and management of cardiomyopathies in cats. *J Vet Intern Med*. 2020;**34**(3):1062–1077.

62. Luis Fuentes V, Wilkie LJ. Asymptomatic hypertrophic cardiomyopathy: diagnosis and therapy. *Vet Clin North Am Small Anim Pract*. 2017;**47**(5):1041–1054.

63. Maleszewski JJ, Lai CK, Veinot JP. Anatomic considerations and examination of cardiovascular specimens (excluding devices). In: Buja LM, Butany J, eds. *Cardiovascular Pathology*. 4th ed. Academic Press; 2016:1–56.

64. Marino F, Scalise M, Cianflone E, et al. Role of c-Kit in myocardial regeneration and aging. *Front Endocrinol (Lausanne)*. 2019;**10**:371.

65. Marketou ME, Parthenakis FI, Kalyva A, et al. Circulating mesenchymal stem cells in patients with hypertrophic cardiomyopathy. *Cardiovasc Pathol*. 2015;**24**(3):149–153.

66. Marvasti TB, Alibhai FJ, Weisel RD, et al. CD34(+) stem cells: promising roles in cardiac repair and regeneration. *Can J Cardiol*. 2019;**35**(10):1311–1321.

67. Meurs KM, Norgard MM, Ederer MM, et al. A substitution mutation in the myosin binding protein C gene in ragdoll hypertrophic cardiomyopathy. *Genomics*. 2007;**90**(2):261–264.

68. Meurs KM, Sanchez X, David RM, et al. A cardiac myosin binding protein C mutation in the Maine Coon cat with familial hypertrophic cardiomyopathy. *Hum Mol Genet*. 2005;**14**(23):3587–3593.

69. Miettinen M, Lasota J. KIT (CD117): a review on expression in normal and neoplastic tissues, and mutations and their clinicopathologic correlation. *Appl Immunohistochem Mol Morphol*. 2005;**13**(3):205–220.

70. Mitsui K, Tokuzawa Y, Itoh H, et al. The homeoprotein Nanog is required for maintenance of pluripotency in mouse epiblast and ES cells. *Cell*. 2003;**113**(5):631–642.

71. Muhlfeld C, Nyengaard JR, Mayhew TM. A review of state-of-the-art stereology for better quantitative 3D morphology in cardiac research. *Cardiovasc Pathol*. 2010;**19**(2):65–82.

72. Nakamura R, Yabuki A, Ichii O, et al. Changes in renal peritubular capillaries in canine and feline chronic kidney disease. *J Comp Pathol*. 2018;**160**:79–83.

73. Nascimento C, Gameiro A, Ferreira J, et al. Diagnostic value of VEGF-A, VEGFR-1 and VEGFR-2 in feline mammary carcinoma. *Cancers (Basel)*. 2021;**13**(1):117.

74. Nielsen JS, McNagny KM. Novel functions of the CD34 family. *J Cell Sci*. 2008;**121**(Pt 22):3683–3692.

75. Novo Matos J, Pereira N, Glaus T, et al. Transient myocardial thickening in cats associated with heart failure. *J Vet Intern Med*. 2018;**32**(1):48–56.

76. Paige CF, Abbott JA, Elvinger F, et al. Prevalence of cardiomyopathy in apparently healthy cats. *J Am Vet Med Assoc*. 2009;**234**(11):1398–1403.

77. Pang LY, Bergkvist GT, Cervantes-Arias A, et al. Identification of tumour initiating cells in feline head and neck squamous cell carcinoma and evidence for gefitinib induced epithelial to mesenchymal transition. *Vet J*. 2012;**193**(1):46–52.

78. Pang LY, Blacking TM, Else RW, et al. Feline mammary carcinoma stem cells are tumorigenic, radioresistant, chemoresistant and defective in activation of the ATM/p53 DNA damage pathway. *Vet J*. 2013;**196**(3):414–423.

79. Payne J, Luis Fuentes V, Boswood A, et al. Population characteristics and survival in 127 referred cats with hypertrophic cardiomyopathy (1997 to 2005). *J Small Anim Pract*. 2010;**51**(10):540–547.

80. Payne JR, Borgeat K, Brodbelt DC, et al. Risk factors associated with sudden death vs. congestive heart failure or arterial thromboembolism in cats with hypertrophic cardiomyopathy. *J Vet Cardiol*. 2015;**17**(suppl 1):S318–S328.

81. Payne JR, Borgeat K, Connolly DJ, et al. Prognostic indicators in cats with hypertrophic cardiomyopathy. *J Vet Intern Med*. 2013;**27**(6):1427–1436.

82. Payne JR, Brodbelt DC, Luis Fuentes V. Cardiomyopathy prevalence in 780 apparently healthy cats in rehoming centres (the CatScan study). *J Vet Cardiol*. 2015;**17**(suppl 1):S244–S257.

83. Phadke RS, Vaideeswar P, Mittal B, et al. Hypertrophic cardiomyopathy: an autopsy analysis of 14 cases. *J Postgrad Med*. 2001;**47**(3):165–170.

84. Robinson WF, Robinson NA. Cardiovascular system. In: Maxie MG, ed. *Jubb, Kennedy, and Palmer's Pathology of Domestic Animals*. 6th ed. Elsevier; 2016:1–101.

85. Rosc-Schluter BI, Hauselmann SP, Lorenz V, et al. NOX2-derived reactive oxygen species are crucial for CD29-induced pro-survival signalling in cardiomyocytes. *Cardiovasc Res*. 2012;**93**(3):454–462.

86. Ross RS. The extracellular connections: the role of integrins in myocardial remodeling. *J Card Fail*. 2002;**8**(6 suppl):S326–S331.

87. Rutigliano L, Corradetti B, Valentini L, et al. Molecular characterization and in vitro differentiation of feline progenitor-like amniotic epithelial cells. *Stem Cell Res Ther*. 2013;**4**(5):133.

88. Schipper T, Van Poucke M, Sonck L, et al. A feline orthologue of the human MYH7 c.5647G>A (p.(Glu1883Lys)) variant causes hypertrophic cardiomyopathy in a domestic shorthair cat. *Eur J Hum Genet*. 2019;**27**(11):1724–1730.

89. Seta N, Kuwana M. Derivation of multipotent progenitors from human circulating CD14+ monocytes. *Exp Hematol*. 2010;**38**(7):557–563.

90. Sidney LE, Branch MJ, Dunphy SE, et al. Concise review: evidence for CD34 as a common marker for diverse progenitors. *Stem Cells*. 2014;**32**(6):1380–1389.

91. Simons M, Gordon E, Claesson-Welsh L. Mechanisms and regulation of endothelial VEGF receptor signalling. *Nat Rev Mol Cell Biol*. 2016;**17**(10):611–625.

92. Stríz I, Trebichavský I. Calprotectin—a pleiotropic molecule in acute and chronic inflammation. *Physiol Res*. 2004;**53**(3):245–253.

93. Taghavi S, Sharp TE 3rd, Duran JM, et al. Autologous c-Kit+ mesenchymal stem cell Injections provide superior therapeutic benefit as compared to c-Kit+ cardiac-derived stem cells in a feline model of isoproterenol-induced cardiomyopathy. *Clin Transl Sci*. 2015;**8**(5):425–431.

94. Tallquist MD, Molkentin JD. Redefining the identity of cardiac fibroblasts. *Nat Rev Cardiol*. 2017;**14**(8):484–491.

95. Tantin D. Oct transcription factors in development and stem cells: insights and mechanisms. *Development*. 2013;**140**(14):2857–2866.

96. Treggiari E, Ressel L, Polton GA, et al. Clinical outcome, PDGFRβ and KIT expression in feline histiocytic disorders: a multicentre study. *Vet Comp Oncol*. 2017;**15**(1):65–77.

97. Urbich C, Dimmeler S. Endothelial progenitor cells: characterization and role in vascular biology. *Circ Res*. 2004;**95**(4):343–353.

98. Van Vleet JF, Ferrans VJ, Weirich WE. Pathologic alterations in hypertrophic and congestive cardiomyopathy of cats. *Am J Vet Res*. 1980;**41**(12):2037–2048.

99. Willett BJ, Cannon CA, Hosie MJ. Expression of CXCR4 on feline peripheral blood mononuclear cells: effect of feline immunodeficiency virus infection. *J Virol*. 2003;**77**(1):709–712.

100. Willey CD, Balasubramanian S, Rodríguez Rosas MC, et al. Focal complex formation in adult cardiomyocytes is accompanied by the activation of beta3 integrin and c-Src. *J Mol Cell Cardiol*. 2003;**35**(6):671–683.

101. Yadav SK, Mishra PK. Isolation, characterization, and differentiation of cardiac stem cells from the adult mouse heart. *J Vis Exp*. 2019;(143):10.3791/58448. doi:10.3791/58448.

102. Yannarelli G, Pacienza N, Montanari S, et al. OCT4 expression mediates partial cardiomyocyte reprogramming of mesenchymal stromal cells. *PLoS One*. 2017;**12**(12):e0189131.

103. Yogalingam G, Anson DS. Molecular cloning of feline CD34. *Vet Immunol Immunopathol*. 2003;**95**(1-2):53–61.

104. Zhou B, Wu SM. Reassessment of c-Kit in cardiac cells: a complex interplay between expression, fate, and function. *Circ Res*. 2018;**123**(1):9–11.

105. Zhou R, Comizzoli P, Keefer CL. Endogenous pluripotent factor expression after reprogramming cat fetal fibroblasts using inducible transcription factors. *Mol Reprod Dev*. 2019;**86**(11):1671–1681.